Evaluation of Fuller's earth for the adsorption of mercury from aqueous solutions: A comparative study with activated carbon

John U. Kennedy Oubagaranadin [a], N. Sathyamurthy [b], Z.V.P. Murthy [c,*]

[a] *Department of Ceramic and Cement Technology, PDA College of Engineering, Gulbarga 585102, Karnataka, India*
[b] *Department of Chemical Engineering, A.C. College of Technology, Anna University, Chennai 600025, Tamil Nadu, India*
[c] *Department of Chemical Engineering, S.V. National Institute of Technology, Surat 395007, Gujarat, India*

Abstract

Fuller's earth (FE) has been used as an adsorbent in this work to remove mercury from aqueous solutions. For the purpose of comparison, simultaneous experiments using activated carbon (AC) have also been done. The aim of the work is to test how best FE can be used as an adsorbent for mercury. Equilibrium isotherms, such as Freundlich, Langmuir, Dubinin–Redushkevich, Temkin, Harkins–Jura, Halsey and Henderson have been tested. Kinetic studies based on Lagergren first-order, pseudo-second-order rate expressions and intra-particle diffusion studies have been done. The batch experiments were conducted at room temperature (30 °C) and at the normal pH (6.7 ± 0.2) of the solution. It has been observed that Hg(II) removal rate is better for FE than AC, due to large dosage requirement, whereas the adsorption capacity of AC is found to be much better than FE. Hence, although FE can be used as an adsorbent, a high dosage is required, when compared to AC. Hybrid fractional error function analysis shows that the best-fit for the adsorption equilibrium data is represented by Freundlich isotherm. Kinetic and film diffusion studies show that the adsorption of mercury on FE and AC is both intra-particle diffusion and film diffusion controlled.
© 2006 Elsevier B.V. All rights reserved.

Keywords: Fuller's earth; Adsorption; Mercury; Wastewater treatment; Isotherms; Kinetics

1. Introduction

Fuller's earth is a type of sedimentary clay having high magnesium oxide content, used in bleaching and clarifying petroleum and in refining edible oils. As a naturally occurring adsorbent material, it can be tested to remove heavy metals from wastewaters, which if released untreated can pose a number of health problems to the human kind. Mercury has been chosen in this work for experimentation. Among several methods for the removal of heavy metals from solutions (precipitation, evaporation, electroplating, ion exchange and membrane separation), adsorption proves to be an efficient and cost effective method [1–15]. In the present study, adsorption of mercury on FE and AC has been studied at the normal pH (6.7 ± 0.2) of the solution and at room temperature (30 °C). Number of works on the removal of mercury using activated carbon had been reported [105–119], whereas work on heavy metals removal by adsorption using Fuller's earth is feeble. This investigation was aimed, in addition to find the adsorption capability of FE for mercury, to test the validity of batch experimental data to various two-parameter adsorption isotherm models such as Freundlich [16], Langmuir [17–19], Dubinin–Redushkevich [20,21], Temkin [22], Harkins–Jura [23,24], Halsey [25] and Henderson [26].

2. Experimental

2.1. Materials and methods

The chemicals used were mercury (II) chloride (Merck), potassium iodide (BDH), potassium hydrogen phthalate (BDH), sodium thiosulphate (SD Fine), gelatin (SD Fine), Fuller's earth (Loba Chemie, India) and activated carbon (Merck). Specifications of Fuller's earth [120] and activated carbon are given in Tables 1 and 2, respectively. The surface area of AC and FE used are 1250 m²/g and 120–140 m²/g, respectively. A double

Nomenclature

AC	activated carbon
B	constant in D–R adsorption model (mol^2/J^2)
B_1	constant in Temkin adsorption isotherm ($=RT/b$) (mg/g)
C_0	initial concentration of adsorbate in solution (mg/L)
C_e	equilibrium concentration of adsorbate in solution (mg/L)
C_t	adsorbate concentration in solution at time t
e	Polanyi potential (J/mol)
E	mean free energy (J/mol)
F	fractional attainment of equilibrium
FE	Fuller's earth
k_1	Lagergren's first-order adsorption rate constant (min^{-1})
k_2	second-order adsorption rate constant (g/mg min)
k_{fd}	film diffusion rate constant (min^{-1})
K_F	Freundlich constant (L/g)
k_{ip}	intraparticle diffusion constant ($mg/g\,min^{0.5}$)
K_L	Langmuir constant (L/mg)
K_T	Temkin constant (L/mg)
n	exponent in Freundlich isotherm
N	number of experimental data points
p	number of parameters in the adsorption isotherm
q_e	amount of adsorbate adsorbed at equilibrium (mg/g)
q_m	monolayer adsorption capacity (mg/g), mol/g in D–R adsorption model
q_t	amount of adsorbate adsorbed at time t (mg/g)
R	universal gas constant (8.314 J/mol K)
R_L	Langmuir separation factor
t	time (min)
T	absolute temperature (K)

beam UV–vis spectrophotometer (HITACHI U2000 Model) was used to determine the residual Hg(II) concentration in solutions [27].

2.2. Spectrophotometric determination of Hg(II)

The formation of a pink colored product when rhodamine 6G is treated with tetraiodomercurate(II) is used to determine mercury (10–50 μg) in a final volume of 50 mL. It is reported [27] that the reaction occurs immediately over the pH range 1–7 and when the system is stabilized with gelatin, the absorbance remains unchanged at 575 nm for atleast 24 h.

2.3. Adsorption experiments

2.3.1. Equilibrium studies

(i) 100 mL solutions of 50 mg/L Hg(II) concentration each were treated with 2.5, 5.0, 7.5, 10.0, 12.5, and 15.0 g of

Table 1
Specifications of Fuller's earth

Chemical composition	
SiO_2	71.27%
Al_2O_3	12.56%
Fe_2O_3	5.40%
MgO	2.13%
TiO_2	1.94%
K_2O	1.22%
CaO	0.69%
MnO	0.06%
P_2O_5	0.03%
Ba	0.04%
Cr	0.019%
LOI	18.58%
Impurities	Rutile, quartz, feldspar
Physical property	
Surface area	120–140 m^2/g
Porosity	60–70%
Cation exchange capacity	50–200 meq/100 g
Mean equivalent pore diameter	190–200 Å
Point of zero charge of edge face	7.0
Particle size	10 μm
Particle density	0.8 g/cm^3

FE, respectively, and equilibrated for a period of 24 h at room temperature (30 °C) and at a pH of 6.7 ± 0.2 of the solution in an orbital flask shaker.

(ii) 100 mL solutions of 50 mg/L Hg(II) concentration each were treated with 30, 60, 90, 120, 150, 180, 210, 250, and 300 mg of AC, respectively, and equilibrated for a period

Table 2
Specifications/properties of activated carbon

	Value
Specification	
Substances soluble in nitric acid	$\leq$1%
Water-soluble matter	$\leq$0.5%
Substances soluble in ethanol	$\leq$0.2%
Sulphate (SO_4)	$\leq$100 ppm
Iron (Fe)	$\leq$300 ppm
Lead (Pb)	$\leq$10 ppm
Zinc (Zn)	$\leq$10 ppm
Residue on ignition (600 °C)	$\leq$1%
Porosity	70–80%
Combustible	96.5%
Property	
pH_{zpc}	5.7
Cation exchange capacity	0.75 meq/g
Surface area	1250 m^2/g
Average particle size	104 μm
Particle density	0.777 g/cm^3
Surface acid groups (meq/g)	
(I) Carboxyl	1.2
(II) Lactonic	1.8
(III) Phenolic	0.9
(IV) Carbonyl	1.6
Total basic groups	1.1 meq/g
Decolorizing power	55.5 mg/g
Particle size range	−65 + Pan (Tyler STD)

Table 3
Batch experimental data for the adsorption of Hg(II) on FE and AC, at normal pH and at room temperature (30 °C)

Equilibrium studies				Optimum dosage				Effect of contact time			
Activated carbon		Fuller's earth		Activated carbon		Fuller's earth		Activated carbon		Fuller's earth	
q_e (mg/g)	C_e (mg/L)	q_e (mg/g)	C_e (mg/L)	Dosage (g)	%Hg(II) removed	Dosage (g)	%Hg(II) removed	Time (min)	q_t (mg/g)	Time (min)	q_t (mg/g)
57.33	32.8	1.044	23.9	0.050	39.8	2.0	41.8	5	10.939	5	0.4602
46.10	22.4	0.820	9.0	0.100	54.8	5.0	66.8	10	10.987	10	0.4634
39.78	14.2	0.607	4.5	0.150	68.8	9.0	88.2	20	11.104	20	0.4680
33.17	10.2	0.480	2.0	0.200	77.6	14.0	97.4	30	11.198	30	0.4703
28.33	7.5	0.390	1.2	0.300	85.8	20.0	99.8	40	11.284	45	0.4721
24.50	5.9	0.329	0.7	0.400	91.1	–	–	50	11.362	60	0.4730
21.67	4.5	–	–	0.500	94.1	–	–	90	11.626	90	0.4748
18.60	3.5	–	–	0.600	96.1	–	–	–	–	–	–
15.87	2.4	–	–	–	–	–	–	–	–	–	–
12.20	1.3	–	–	–	–	–	–	–	–	–	–

of 24 h at room temperature and at a pH of 6.7 ± 0.2 of the solution in an orbital flask shaker.

The solutions were then filtered and the residual Hg(II) concentrations determined spectrophotometrically.

2.3.2. Determination of optimum dosage

(i) 100 mL solutions of 50 mg/L Hg(II) concentration each were treated with 2, 5, 9, 14, and 20 g of FE, respectively and shaken for a period of 1 h at room temperature (30 °C) and at a pH of 6.7 ± 0.2 of the solution.
(ii) 100 mL solutions of 50 mg/L Hg(II) concentration each were treated with 50, 100, 150, 200, 300, 400, 500, and 600 mg of AC and shaken for period of 1 h at room temperature (30 °C) and at a pH of 6.7 ± 0.2 of the solution.

2.3.3. Effect of contact time

(i) 100 mL of 50 mg/L Hg(II) concentration solutions were treated with 10 g (optimum dosage) of FE for 5, 10, 20, 30, 45, 60, and 90 min.

(ii) 100 mL of 50 mg/L Hg(II) concentration solutions were treated with 400 mg of AC for 5, 10, 20, 30, 40, 50, and 90 min.

3. Results and discussion

3.1. Equilibrium studies

The experimental data (Table 3) on equilibrium studies for the adsorption of Hg(II) on FE and AC were tested to fit the various 2-parameter adsorption isotherm models. Linearized forms of the various adsorption isotherms, the values of parameters involved and the correlation coefficients are given in Table 4.

3.1.1. Freundlich model

This model often gives a better fit particularly for adsorption from liquids and can be expressed as:

$$q_e = K_F C_e^{1/n} \tag{1}$$

where q_e (mg/g) is the amount of adsorbate adsorbed at equilibrium and C_e (mg/L) is the equilibrium concentration of adsorbate

Table 4
Two-parameter adsorption isotherm models and parameter values of the isotherms for the adsorption of Hg(II) on Fuller's earth and activated carbon at normal pH of the solution and at room temperature (30 °C)

| Model	Linearized equation	Parameters values for the adsorption of Hg(II) on	
		Fuller's earth	Activated carbon
Freundlich	$\log q_e = \log K_F + \frac{1}{n}\log C_e$	$K_F = 0.373$; $\frac{1}{n} = 0.334$; $R^2 = 0.996$	$K_F = 10.464$; $\frac{1}{n} = 0.487$; $R^2 = 0.997$
Langmuir	$\frac{C_e}{q_e} = \frac{1}{q_m K_L} + \frac{C_e}{q_m}$	$K_L = 0.359$; $q_m = 1.145$; $R^2 = 0.991$; $R_L = 0.053$	$K_L = 0.104$; $q_m = 69.44$; $R^2 = 0.967$; $R_L = 0.161$
Dubinin–Redushkevich (D–R)	$\ln q_e = \ln q_m - B\varepsilon^2$	$B = 2 \times 10^{-9}$; $q_m = 1.84 \times 10^{-5}$; $E = 15811$; $R^2 = 0.9955$	$B = 4 \times 10^{-9}$; $q_m = 1.59 \times 10^{-3}$; $E = 11180$; $R^2 = 0.9928$
Temkin	$q_e = B_1 \ln K_T + B_1 \ln C_e$	$K_T = 5.675$; $B_1 = 0.206$; $R^2 = 0.981$	$K_T = 1.23$; $B_1 = 13.951$; $R^2 = 0.949$
Harkins–Jura	$\frac{1}{q_e^2} = \left[\frac{B}{A}\right] - \left[\frac{1}{A}\right]\log C_e$	$A = 0.189$; $B = 1.331$ $R^2 = 0.893$	$A = 238.1$; $B = 1.333$; $R^2 = 0.836$
Halsey	$\ln q_e = \left[\left(\frac{1}{n}\right)\ln k\right] - \left(\frac{1}{n}\right)\ln C_e$	$n = -2.99$; $k = 19.05$; $R^2 = 0.995$	$n = -2.05$; $k = 8.08 \times 10^{-3}$; $R^2 = 0.997$
Henderson	$\ln[-\ln(1 - C_e)] = \ln k + n \ln q_e$	$n = 966091$; $k = 9 \times 10^{-7}$; $R^2 = 0.976$	$n = 2.04$; $k = 2907.4$; $R^2 = 0.9975$
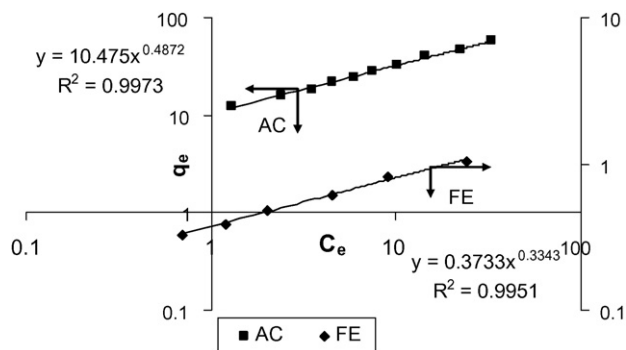
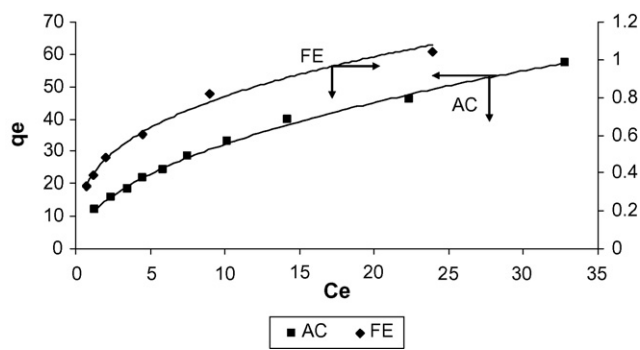Fig. 1. Freundlich plots.

in solution. Many researchers have used this model to interpret their sorption data for various systems [28–61]. In this model, the mechanism and the rate of adsorption are functions of the constants $1/n$ and K_F (L/g). The plots for the adsorption of Hg(II) on FE and AC are shown in Fig. 1. The plots give good fit (correlation coefficient, $R^2 = 0.996$ for FE and 0.997 for AC). For a good adsorbent, $0.2 < 1/n < 0.8$. A smaller value of $1/n$ indicates better adsorption and formation of relatively strong bond between the adsorbate and adsorbent. From the $1/n$ values (see Table 4), it is observed that FE adsorbs Hg(II) stronger than AC.

3.1.2. Langmuir model

The Langmuir adsorption isotherm is given by the following equation:

$$q_e = \frac{q_m K_L C_e}{1 + K_L C_e} \tag{2}$$

A host of research workers have applied this model to interpret their sorption data [28–83]. In the present work, we find that the plots shown in Fig. 2 for both FE and AC give a fairly good fit ($R^2 = 0.991$ for FE and 0.967 for AC) for the present experimental data. In the model, q_m (mg/g) is the amount of adsorption corresponding to complete monolayer coverage, i.e., the maximum adsorption capacity and K_L (L/mg) is the Langmuir constant. From the values of q_m (see Table 4), it is observed that the maximum adsorption capacity of AC is much better (≈ 60 times) than that of FE. This is due to the low specific surface area of FE. Hence, a high dosage of FE is required. However, adsorption capacity of the adsorbents may be improved by thermal activation before usage. For Langmuir type adsorption process,
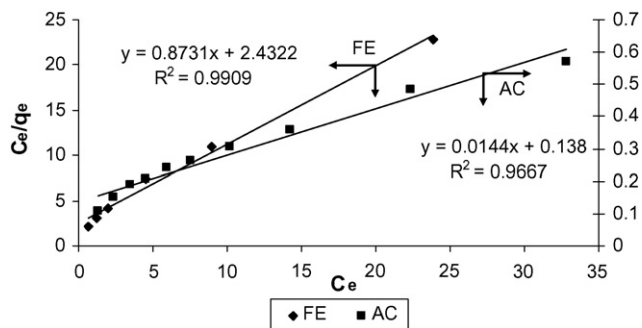

Fig. 2. Langmuir plots.

to determine if the adsorption is favorable or not, a dimensionless separation factor is defined as:

$$R_L = \frac{1}{1 + K_L C_0} \tag{3}$$

If $R_L > 1$, the isotherm is unfavorable, $R_L = 1$, the isotherm is linear, $0 < R_L < 1$, the isotherm is favorable, $R_L = 0$, the isotherm is irreversible.

The R_L values for both FE and AC fall between 0 and 1 (see Table 4), indicating that the isotherms are favorable. Fig. 3 shows a plot of residual equilibrium concentration C_e (mg/L) against adsorbate loading q_e (mg/g). The curves are convex upward and so they are favorable because a relatively high adsorbate loading may be obtained at low concentration in the solution.

3.1.3. Dubinin–Redushkevich (D–R) model

This adsorption isotherm is given as:

$$q_e = q_m \exp(-Be^2) \tag{4}$$

where q_m (mol/g) is the theoretical monolayer saturation capacity of the adsorbent and e (known as Polanyi potential) is given as:

$$e = RT \ln\left(1 + \frac{1}{C_e}\right) \tag{5}$$

The constant B (mol²/J²) given by the following equation [84], the mean free energy E (J/mol) of adsorption per molecule of adsorbate, when it is transferred to the surface of the solid from infinity in the solution, is

$$E = \frac{1}{\sqrt{2B}} \tag{6}$$

The linear form of D–R equation is:

$$\ln q_e = \ln q_m - Be^2 \tag{7}$$

A plot of $\ln q_e$ versus e^2 should yield a straight line. This plot for the present experimental data is shown in Fig. 4. The fits are good in the present study ($R^2 = 0.9955$ for FE and 0.9928 for AC). The values of the parameter E (see Table 4) for FE are found to be more than that for AC. Also, the theoretical monolayer saturation capacity for AC is much better (≈ 85 times) than FE. Hence, a high dosage of FE is required.

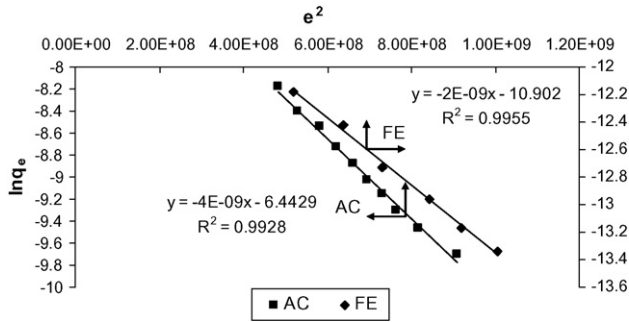Fig. 3. Favorable isotherms.

Fig. 4. Dubinin–Redushkevich plots.

3.1.4. Temkin model

The Temkin adsorption isotherm is expressed as:

$$q_e = \frac{RT}{b}\ln(K_T C_e) \tag{8}$$

The linearized form of the above equation is:

$$q_e = B_1 \ln K_T + B_1 \ln C_e \tag{9}$$

where $B_1 = RT/b$; R is the universal gas constant (8.314 J/mol K) and T is the absolute temperature (K).

Temkin isotherm takes into account the adsorbing species–adsorbent interactions. A plot of q_e versus $\ln C_e$ yields a straight line (Fig. 5) from which the isotherm constants B_1 and K_T (L/mg) can be determined. K_T is the equilibrium binding constant corresponding to the maximum binding energy and constant B_1 is related to the heat of adsorption. From the values of K_T (see Table 4) it may be observed that the binding energy is better for FE than AC as evinced by the Freundlich model, whereas the heat of adsorption is more for AC than FE.

3.1.5. Harkins–Jura model

The plots for the experimental data, using this model, are shown in Fig. 6. This model accounts for multilayer adsorption and also for the existence of heterogeneous pore distribution in the adsorbent. A low value of R^2 for both FE (0.893) and AC (0.836) indicates that the adsorption process follow fairly this model.
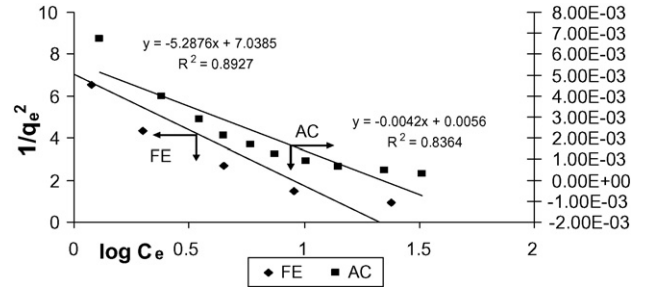

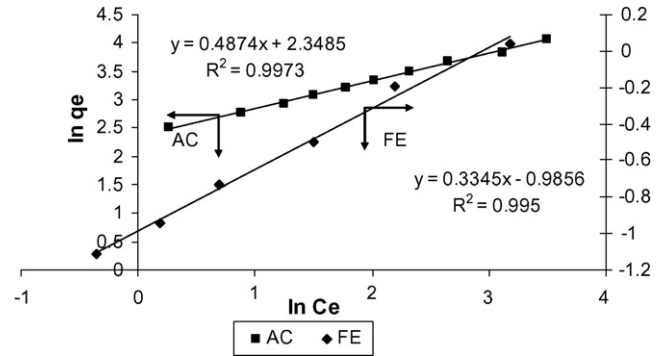Fig. 5. Temkin plots.

Fig. 6. Harkins–Jura plots.

Fig. 7. Halsey plots.

3.1.6. Halsey and Henderson model

These models explain multilayer adsorption [85]. The experimental data shown through Figs. 7 and 8 gives good correlation coefficients for these models, confirming multilayer adsorption of Hg(II) on FE and AC.

3.1.7. Best-fit isotherm model

All the isotherms studied in this work are in their linearized form. Due to the inherent bias resulting from linearization, to find out the best-fit isotherm model to the experimental equilibrium data, the hybrid fractional error function [121] of non-linear regression is employed, as it compensates for low concentrations by balancing absolute deviation against fractional error and is more reliable than other error functions [122]. The hybrid error is given as:

$$\text{HYBRID} = \frac{100}{N-p}\sum\left[\frac{q_{e,exp} - q_{e,calc}}{q_{e,exp}}\right]_i \tag{10}$$
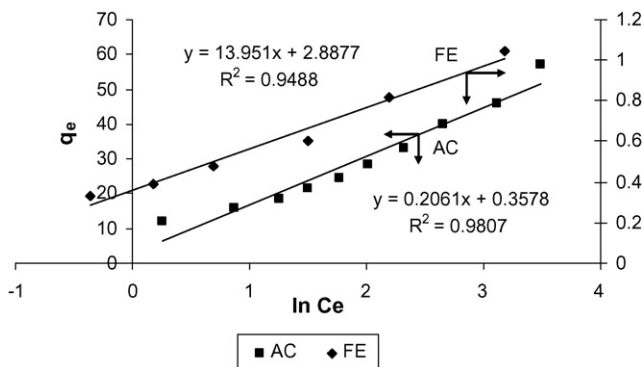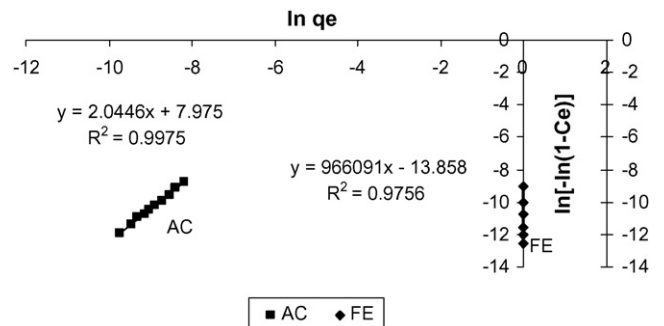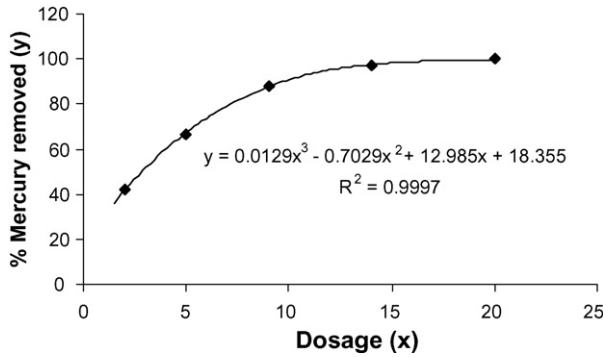

Fig. 8. Henderson plots.

Fig. 9. Percentage Hg(II) removal with increase in FE dosage.

where N is the number of data points and p is the number of parameters in the isotherm model. The hybrid error is lowest for Freundlich model for adsorption on both AC (0.013) and FE (0.134) and hence the best-fit is the Freundlich adsorption isotherm.

3.2. Optimum dosage

Figs. 9 and 10 show the plots of percentage of Hg(II) removed versus adsorbent dosage. Approximately above 10 g of FE and near 0.4 g of AC dosage, the percentage of Hg(II) removed almost stabilizes. Hence, the optimum dosage is taken as 10 g for FE and 0.4 g for AC.

3.3. Effect of contact time

The rate at which the metal ion is removed from solution by the adsorbent is a significant factor for the utilization of the process in the treatment of effluents. The data on the effect of contact time is interpreted under (i) rate constant study and (ii) intra-particle diffusion study.

3.3.1. Rate constant study

The rate constant for surface adsorption of the Hg(II) ion on FE and AC is studied under the light of the pseudo-first-order rate expression of Lagergren model [86,87] and the pseudo-second-order kinetic rate expression of Ho and McKay [88–98].

The integrated form of the Lagergren equation is given by

$$\log[q_e - q_t] = \log q_e - \frac{k_1}{2.303}t \tag{11}$$
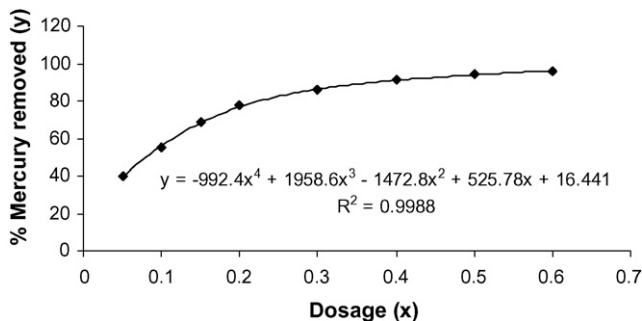

Fig. 10. Percentage Hg(II) removal with increase in AC dosage.
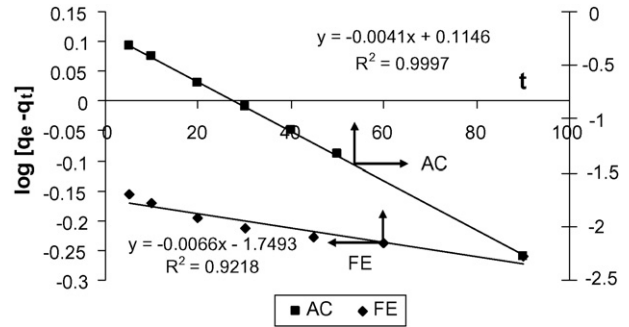

Fig. 11. Pseudo first-order kinetic plots.

A plot of Eq. (11) is shown in Fig. 11 for FE and AC. The experimental data gives good fit for both FE ($R^2 = 0.922$) and AC ($R^2 = 0.999$) indicating that the Lagergren model is applicable, although better for AC. The values of the first-order rate constants ($k_1 = 0.015 \text{ min}^{-1}$ for FE and 0.0094 min^{-1} for AC) indicate that adsorption is faster in FE than AC.

The pseudo second-order kinetic rate expression in the integrated form is:

$$\frac{t}{q_t} = \frac{1}{k_2 q_e^2} + \frac{t}{q_e} \tag{12}$$

The plot for the above equation is shown in Fig. 12. The data gives perfect fit for this model for both FE ($R^2 = 0.999$) and AC ($R^2 = 1$). The values of the second-order rate constant found from the slopes of the plots for FE ($k_2 = 7.23 \text{ g/mg min}$) and AC ($k_2 = 0.094 \text{ g/mg min}$) indicate that Hg(II) removal rate is faster by FE than AC.

3.3.2. Intra-particle diffusion study

Besides adsorption at the outer surface of the adsorbent, there is also a possibility of intra-particle diffusion of the metal ion from the bulk of the outer surface into the pores of the adsorbent material. This possibility is studied by plotting q_t versus $t^{0.5}$ [99–104]. The plot shown in Fig. 13 presents multi-linearity for FE, indicating that a few steps are taking place. The first linear portion is attributed to the diffusion of adsorbate through the solution to the external surface of adsorbent or the boundary layer (film) diffusion of solute molecules. The second portion describes the gradual adsorption stage, where intra-particle diffusion is rate limiting. The third portion is
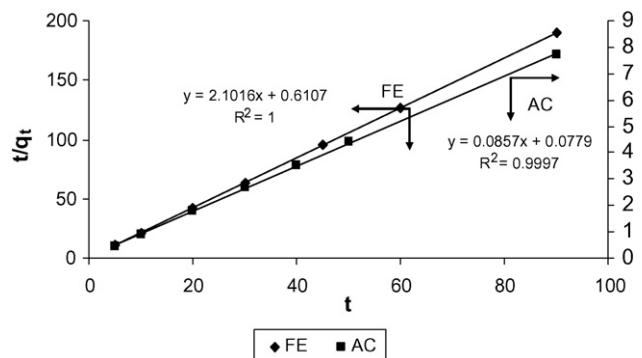

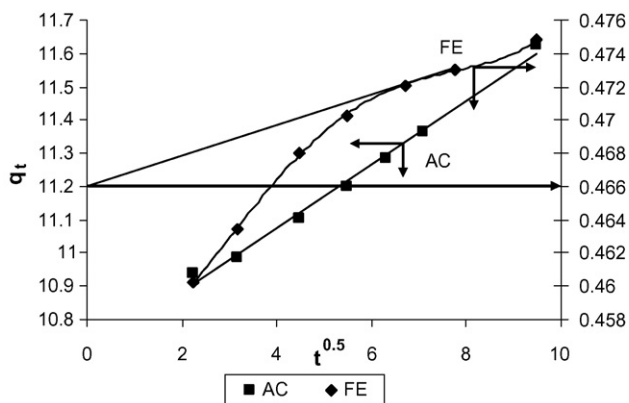Fig. 12. Pseudo-second-order kinetic plots.

Fig. 13. Intraparticle diffusion plot-1.

Fig. 15. Liquid film diffusion plot.

attributed to the final equilibrium stage for which the intra-particle diffusion starts to slow down due to the extremely low adsorbate concentration left in the solution. The value of the intra-particle diffusion rate constant found from the slope, k_{ip}, is 9×10^{-4} mg/g min$^{0.5}$.

The plot for AC although is not multi-linear, it is linear ($R^2 = 0.992$), indicating the existence of intra-particle diffusion. For adsorption on AC, $k_{ip} = 0.096$ mg/g min$^{0.5}$.

Further confirmation to the occurrence of intra-particle diffusion is obtained from a plot of log (q_t) versus log (t) (see Fig. 14). The plots give a linear fit ($R^2 = 0.991$ for FE and $R^2 = 0.906$ for AC) indicating intra-particle diffusion is taking place. The values of the slope calculated from the plots are 0.0111 for FE and 0.0198 for AC. These values are widely divergent from the value of 0.5, which corresponds to the intra-particle diffusion being rate determining [104]. The divergence in value from 0.5 indicates that besides intra-particle diffusion, there may be other processes controlling the rate, all operating simultaneously.

3.4. Mass-transfer studies

The experimental conditions for the batch kinetic tests are: volume of Hg(II) solution – 100 mL of 50 mg/L concentration; temperature – 303 K; pH of the solution – 6.7 ± 0.2; rpm of the rotary shaker – 180; adsorbent dosage – 0.4 g AC, 10 g FE.
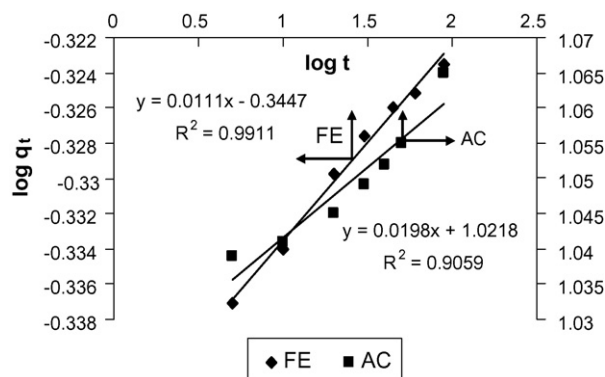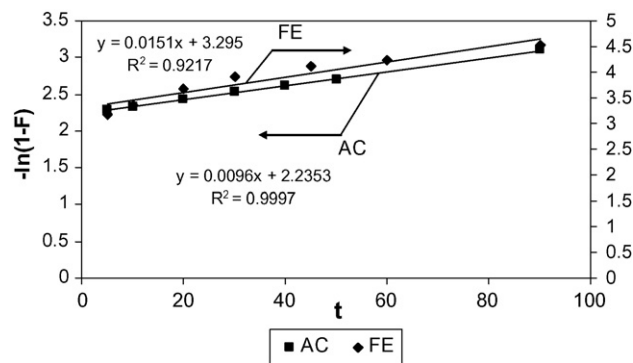

Fig. 14. Intraparticle diffusion plot-2.

3.4.1. Film diffusion

When the transport of the solute molecules from the liquid phase to the solid phase boundary plays a most significant role in adsorption, the liquid film diffusion model [123] can be applied:

$$\ln (1 - F) = -k_{fd}t \tag{13}$$

where F is the fractional attainment of equilibrium ($F = q_t/q_e$), and k_{fd} is the film diffusion rate constant. A linear plot of $-\ln (1 - F)$ versus t with zero intercept would suggest that the kinetics of the adsorption process is primarily controlled by diffusion through the liquid film surrounding the solid adsorbents. This plot is shown in Fig. 15 for AC and FE. The straight lines are not passing through the origin, and hence the adsorption process is not primarily film diffusion controlled for both AC and FE. The film diffusion rate constants k_{fd}, calculated from the slopes are 0.0096 min^{-1} and 0.0151 min^{-1} for adsorption AC and FE, respectively.

4. Conclusions

The present study shows that Fuller's earth, like activated carbon, follows the adsorption isotherm models tested; viz. Freundlich, Langmuir, Dubinin–Redushkevich, Halsey and Henderson; except Temkin and Harkins–Jura. However, the best-fit isotherm is the Freundlich isotherm, as determined by hybrid fractional error analysis. Application of Halsey and Henderson models, indicate that the adsorbents are heteroporous in nature, which is a good characteristic of an absorbent. Fuller's earth is better than activated carbon from the point of strong-bond formation between the adsorbent and adsorbate. However, monolayer adsorbate coverage capacity of Fuller's earth is lesser than activated carbon, indicating that a high dosage of Fuller's earth is required, as evinced by the experimental data. As the adsorption capacity is an important factor, AC in this respect proves to be better than FE for the capture of mercury ions. Kinetic data for both Fuller's earth and activated carbon fits well in pseudo-second-order kinetics, confirming the chemisorption of mercury ions, which can also be evinced by energy of adsorption values, determined by D–R isotherm model. The adsorption process on both Fuller's earth and activated carbon is particle-diffusion-controlled to some extent, although they were used in powder form, with existence of external mass transfer at the initial stages.

References

[1] P.A. Brown, S.A. Gill, S.J. Allen, Metal removal from wastewater using peat, Water Res. 34 (2000) 3907–3916.

[2] G. Yan, T. Viraraghavan, Heavy metal removal from aqueous solution by fungus *Mucor rouxii*, Water Res. 37 (2003) 4486–4496.

[3] T.N.C. Dantas, A.A. Dantas Neto, M.C.P.A. Moura, Removal of chromium from aqueous solutions by diatomite treated with microemulsion, Water Res. 35 (2001) 2219–2224.

[4] T.N.C. Dantas, A.A. Dantas Neto, M.C.P.A. Moura, E.L. Barros Neto, E.P. Telemaco, Chromium adsorption by chitosan impregnated with microemulsion, Langmuir 17 (2001) 4256–4260.

[5] T.N.C. Dantas, A.A. Dantas Neto, M.C.P.A. Moura, E.L. Barros Neto, K.R. Forte, R.H.L. Leite, Heavy metals extraction by microemulsions, Water Res. 37 (2003) 2709–2717.

[6] V. Boonamnuayvitaya, C. Chaiya, W. Tanthapanichakoon, S. Jarudilokkul, Removal of heavy metals by adsorbent prepared from pyrolyzed coffee residues and clay, Sep. Purif. Technol. 35 (2004) 11–22.

[7] N. Adhoum, L. Monser, N. Bellakhal, J. Belgaied, Treatment of electroplating wastewater containing Cu^{2+}, Zn^{2+} and Cr(VI) by electrocoagulation, J. Hazard. Mater. 112 (2004) 207–213.

[8] G.P. Broom, R.C. Squires, M.P.J. Simpson, I. Martin, The treatment of heavy metal effluents by crossflow microfiltration, J. Membr. Sci. 87 (1994) 219–230.

[9] L. Voges, P. Mark, M. Benjamin, Y. Chang, Use of iron oxides to enhance metal removal in crossflow microfiltration, J. Environ. Eng. 127 (2001) 411–416.

[10] D.-J. Chang, S.-J. Hwang, Removal of metal ions from liquid solutions by crossflow microfiltration, Sep. Sci. Technol. 31 (1996) 1831–1842.

[11] X. Chai, G. Chen, P.-L. Yue, Y. Mi, Pilot scale membrane separation of electroplating wastewater by reverse osmosis, J. Membr. Sci. 123 (1997) 235–242.

[12] Metcalf & Eddy, Wastewater Engineering: Treatment and Reuse, 4th ed., Tata McGraw-Hill, New Delhi, 1995.

[13] Z. Reddad, C. Gerente, Y. Andres, P. Le-Cloirec, Adsorption of several metal ions onto a low-cost biosorbent: kinetic and equilibrium studies, Environ. Sci. Technol. 36 (2002) 2067–2073.

[14] C.L. Lasko, M.P. Hurst, An investigation in to the use of chitosan for removal of soluble silver from industrial wastewater, Environ. Sci. Technol. 33 (1999) 3622–3626.

[15] G.L. Rorrer, T.-Y. Hsien, Synthesis of porous-magnetic chitosan beads for removal of cadmium ions from wastewater, Ind. Eng. Chem. Res. 32 (1993) 2170–2178.

[16] H. Freundlich, Über die adsorption in Lösungen, Z. für Physik. Chem. 57 (1907) 385–470.

[17] I. Langmuir, The constitution and fundamental properties of solids and liquids. I. Solids, J. Am. Chem. Soc. 38 (1916) 2221–2295.

[18] I. Langmuir, The constitution and fundamental properties of solids and liquids. II. Liquids, J. Am. Chem. Soc. 39 (1917) 1848–1906.

[19] I. Langmuir, The adsorption of gases on plane surfaces of glass, mica and platinum, J. Am. Chem. Soc. 40 (1918) 1361–1403.

[20] M.M. Dubinin, L.V. Radushkevich, Equation of the characteristic curve of activated charcoal, Proc. Acad. Sci. Phys. Chem. Sect. USSR 55 (1947) 331–333.

[21] M.M. Dubinin, L.V. Radushkevich, Evaluation of microporous materials with a new isotherm, Doklady Akademii Nauk SSSR 55 (1966) 331.

[22] M.J. Temkin, V. Pyzhev, Recent modifications to Langmuir isotherms, Acta Physiochim USSR 12 (1940) 217.

[23] W.D. Harkins, G. Jura, Surfaces of solids. XIII. A vapor adsorption method for the determination of the area of a solid without the assumption of a molecular area, and the areas occupied by nitrogen and other molecules on the surface of a solid, J. Am. Chem. Soc. 66 (1944) 1366–1377.

[24] W.D. Harkins, G. Jura, An adsorption method for the determination of the area of a solid without the assumption of a molecular area, and the area occupied by nitrogen molecules on the surfaces of solids, J. Chem. Phys. 11 (1943) 431–432.

[25] G. Halsey, Physical adsorption on non-uniform surfaces, J. Chem. Phys. 16 (1948) 931–937.

[26] S.M. Henderson, A basic concept of equilibrium moisture, Agric. Eng. 33 (1952) 29–32.

[27] T.V. Ramakrishna, G. Aravamudan, M. Vijayakumar, Spectrophotometric determination of mercury (II) as the ternary complex with rhodamine 6G and iodide, Anal. Chim. Acta 84 (1976) 369–375.

[28] M. Abdulkarim, F.A. Abu Al-Rub, Adsorption of lead ions from aqueous solution onto activated carbon and chemically-modified activated carbon prepared from date pits, Adsorpt. Sci. Technol. 22 (2004) 119–134.

[29] F.A. Abu Al-Rub, Sorption of lead ions from simulated industrial wastewater onto Jordanian low-grade phosphate, Adsorpt. Sci. Technol. 22 (2004) 165–179.

[30] B. Acemioglu, Adsorption of Congo red from aqueous solution onto calcium-rich fly ash, J. Colloid Interf. Sci. 274 (2004) 371–379.

[31] N. Ahalya, R.D. Kanamadi, T.V. Ramachandra, Biosorption of chromium (VI) from aqueous solutions by the husk of bengal gram (*Cicer arientinum*), Electron. J. Biotechnol. 6 (3) (2005) (ISSN: 0717-3458) This paper is available on line at http://www.ejbiotechnology.info/content/vol6/issue3/full/5.

[32] Z. Aksu, Biosorption of reactive dyes by dried activated sludge: equilibrium and kinetic modelling, Biochem. Eng. J. 7 (2001) 79–84.

[33] Z. Aktas, Adsorption of non-ionic surface active agent on fine coal and lignite, Turk. J. Chem. 25 (2001) 311–321.

[34] S. Al-Asheh, F. Banat, A. Masad, Kinetics and equilibrium sorption studies of 4-nitrophenol on pyrolyzed and activated oil shale residue, Environ. Geol. 45 (2004) 1109–1117.

[35] M.A. Al-Ghouti, M.A.M. Khraisheh, S.J. Allen, M.N. Ahmad, The removal of dyes from textile wastewater: a study of the physical characteristics and adsorption mechanisms of diatomaceous earth, J. Environ. Manage. 69 (2003) 229–238.

[36] W.M. Antunes, A.S. Luna, C.A. Henriques, A.C.A. da Costa, An evaluation of copper biosorption by a brown seaweed under optimized conditions, Electron. J. Biotechnol. 6 (3) (2003) (ISSN: 0717-3458) This paper is available on line at http://www.ejbiotechnology.info/content/vol6/issue3/full/5.

[37] N. Bektas, D. Soysal, Kinetics of phosphate removal using surfactant modified clinoptilolite, Fresenius Environ. Bull. 13 (2004) 366–369.

[38] V.M. Boddu, K. Abburi, J.L. Talbott, E.D. Smith, Removal of hexavalent chromium from wastewater using a new composite chitosan biosorbent, Environ. Sci. Technol. 37 (2003) 4449–4456.

[39] G.Y. Chu, T.Y. Kim, S.Y. Cho, Y. Kang, S.D. Kim, S.J. Kim, Adsorption characteristics of zinc–cyanide complexes by waste brewery biomass, J. Ind. Eng. Chem. 10 (2004) 551–557.

[40] S. Deng, R. Bai, Adsorption and desorption of humic acid on aminated polyacrylonitrile fibers, J. Colloid Interf. Sci. 280 (2004) 36–43.

[41] E. Guibal, C. Milot, J.M. Tobin, Metal-anion sorption by chitosan beads: equilibrium and kinetic studies, Ind. Eng. Chem. Res. 37 (1998) 1454–1463.

[42] E. Guibal, A. Larkin, T. Vincent, J.M. Tobin, Chitosan sorbents for platinum sorption from dilute solutions, Ind. Eng. Chem. Res. 38 (1999) 4011–4022.

[43] Y.S. Ho, G. McKay, Sorption of dye from aqueous solution by peat, Chem. Eng. J. 70 (1998) 115–124.

[44] Y.S. Ho, J.F. Porter, G. McKay, Equilibrium isotherm studies for the sorption of divalent metal ions onto peat: copper nickel and lead single component systems, Water, Air, Soil Pollut. 141 (2002) 1–33.

[45] Y.S. Ho, W.T. Chin, C.S. Hsu, C.I. Huang, Sorption of lead ions from aqueous solution using tree fern as a sorbent, Hydrometallurgy 73 (2004) 55–61.

[46] R. Jalali, H. Ghafourian, Y. Asef, S.J. Davarpanah, S. Sepehr, Removal and recovery of lead using nonliving biomass of marine algae, J. Hazard. Mater. B92 (2002) 253–262.

[47] U. Kumar, M. Bandyopadhyay, Sorption of cadmium from aqueous solution using pretreated rice husk, Bioresour. Technol. 97 (2006) 104–109.

[48] M.M. Nassar, Equilibrium studies on the adsorption of glycine on resin, Adsorpt. Sci. Technol. 8 (1991) 86–94.

[49] S. Netpradit, P. Thiravetyan, S. Towprayoon, Adsorption of three azo reactive dyes by metal hydroxide sludge: effect of temperature, pH, and electrolytes, J. Colloid Interf. Sci. 270 (2004) 255–261.

[50] J. Oscik, Adsorption, Ellis Horwood, New York, 1992.

[51] F. Pagnanelli, F. Beolchini, A.D. Biase, F. Veglio, Effect of equilibrium models in the simulation of heavy metal biosorption in single and two-stage UF/MF membrane reactor systems, Biochem. Eng. J. 15 (2003) 27–35.

[52] L. Ray, S. Paul, D. Bera, P. Chattopadhyay, Bioaccumulation of Pb(II) from aqueous solutions by *Bacillus cereus* M_{16}^1, J. Hazard. Substance Res. 5 (2005) 1–21.

[53] J. Romero-Gonzalez, J.R. Peralta-Videa, E. Rodriguez, M. Delgado, J.L. Gardea-Torresdey, Potencial of *Agave lechuguilla* biomass for Cr(III) removal from aqueous solutions: thermodynamic studies, Bioresour. Technol. 97 (2006) 178–182.

[54] C.N. Sawyer, P.L. McCarty, Chemistry for Environmental Engineering, 4th ed., Tata McGraw-Hill, New Delhi, 2002.

[55] F.L. Slejko, Adsorption Technology, Tall Oaks, New Jersey, 1985.

[56] W.T. Tsai, K.J. Hsien, J.M. Yang, Silica adsorbent prepared from spent diatomaceous earth and its application to removal of dye from aqueous solution, J. Colloid Interf. Sci. 275 (2004) 428–433.

[57] B. Volesky, Z.R. Holan, Biosorption of heavy metals, Biotechnol. Prog. 11 (1995) 235–250.

[58] F.C. Wu, R.L. Tseng, R.S. Juang, Comparisons of porous and adsorption properties of carbons activated by steam and KOH, J. Colloid Interf. Sci. 283 (2005) 49–56.

[59] D. Zhou, L. Zhang, J. Zhou, S. Guo, Cellulose/chitin beads for adsorption of heavy metals in aqueous solution, Water Res. 38 (2004) 2643–2650.

[60] S. Tunali, T. Akar, Zn(II) biosorption properties of *Botrytis cinerea biomasa*, J. Hazard. Mater. B131 (2006) 137–145.

[61] F.J. Rivas, F.J. Beltran, O. Gimeno, J. Frades, F. Carvalho, Adsorption of landfill leachates onto activated carbon: equilibrium and kinetics, J. Hazard. Mater. B131 (2006) 170–178.

[62] J. Aburto, A. Mendez-Orozco, S. Le Borgne, Hydrogels as adsorbents of organosulfur compounds currently found in diesel, Chem. Eng. Process. 43 (2004) 1587–1595.

[63] Y. Al-degs, M.A.M. Khraisheh, M.F. Tutunji, Sorption of lead ions on diatomite and manganese oxides modified diatomite, Water Res. 35 (2001) 3724–3728.

[64] S.J. Allen, Q. Gan, R. Matthews, P.A. Johnson, Comparison of optimised isotherm models for basic dye adsorption by Kudzu, Bioresour. Technol. 88 (2003) 143–152.

[65] D.H. Cho, M.H. Yoo, E.Y. Kim, Biosorption of lead (Pb^{2+}) from aqueous solution by *Rhodotorula aurantiaca*, J. Microbiol. Biotechnol. 14 (2004) 250–255.

[66] E. Demirbas, Adsorption of cobalt (II) ions from aqueous solution onto activated carbon prepared from hazelnut shells, Adsorpt. Sci. Technol. 21 (2003) 951–963.

[67] R.H. Doremus, Water speciation in silicate glasses and melts: Langmuir limited site model, Am. Mineral. 85 (2000) 1674–1680.

[68] W. Fiol, J. Poch, I. Villaescusa, Chromium (VI) uptake by grape stalks wastes encapsulated in calcium alginate beads: equilibrium and kinetics studies, Chem. Speciation Bioavailability 16 (2004) 25–34.

[69] H. Genc, J.C. Tjell, D. McConchie, O. Schuiling, Adsorption of arsenate from water using neutralized red mud, J. Colloid Interf. Sci. 264 (2003) 327–334.

[70] T. Jong, D.L. Parry, Adsorption of Pb(II), Cu(II), Cd(II), Zn(II), Ni(II), and As(V) on bacterially produced metal sulfides, J. Colloid Interf. Sci. 275 (2004) 61–71.

[71] R.S. Juang, J.Y. Cheng, Equilibrium sorption of heavy metals and phosphate from single- and binary-sorbate solutions on goethite, J. Colloid Interf. Sci. 275 (2004) 53–60.

[72] M.A.M. Khraisheh, Y.S. Al-Degs, W.A.M. Mcminn, Remediation of wastewater containing heavy metals using raw and modified diatomite, Chem. Eng. J. 99 (2004) 177–184.

[73] S.J. Kim, K.H. Lim, K.H. Joo, M.J. Lee, S.G. Kil, S.Y. Cho, Removal of heavy metal–cyanide complexes by ion exchange, Korean J. Chem. Eng. 19 (2002) 1078–1084.

[74] A.B. Koltuniewicz, A. Witek, K. Bezak, Efficiency of membrane-sorption integrated processes, J. Membr. Sci. 239 (2004) 129–141.

[75] A.G.S. Prado, J.D. Torres, E.A. Faria, S.C.L. Dias, Comparative adsorption studies of indigo carmine dye on chitin and chitosan, J. Colloid Interf. Sci. 277 (2004) 43–47.

[76] S. Ricordel, S. Taha, I. Cisse, G. Dorange, Heavy metals removal by adsorption onto peanut husks carbon: characterization, kinetic study and modeling, Sep. Purif. Technol. 24 (2001) 389–401.

[77] N. Sakkayawong, P. Thiravetyan, W. Nakbanpote, Adsorption mechanism of synthetic reactive dye wastewater by chitosan, J. Colloid Interf. Sci. 286 (2005) 36–42.

[78] V. Sarin, K.K. Pant, Removal of chromium from industrial waste by using eucalyptus bark, Bioresour. Technol. 97 (2006) 15–20.

[79] R.A. Shawabkeh, M.F. Tutunji, Experimental study and modeling of basic dye sorption by diatomaceous clay, Appl. Clay Sci. 24 (2003) 111–120.

[80] P.X. Sheng, Y.P. Ting, J.P. Chen, L. Hong, Sorption of lead, copper, cadmium, zinc, and nickel by marine algal biomass: characterization of biosorptive capacity and investigation of mechanisms, J. Colloid Interf. Sci. 275 (2004) 131–141.

[81] P.L. Tang, C.K. Lee, K.S. Low, Z. Zainal, Sorption of Cr(VI) and Cu(II) in aqueous solution by ethylenediamine modified rice hull, Environ. Technol. 24 (2003) 1243–1251.

[82] V.J.P. Vilar, C.M.S. Botelho, R.A.R. Boaventura, Equilibrium kinetic modelling of Cd(II) biosorption by algae *Gelidium* and agar extraction algal waste, Water Res. 40 (2006) 291–302.

[83] F.C. Wu, R.L. Tseng, R.S. Juang, Role of pH in metal adsorption from aqueous solutions containing chelating agents on chitosan, Ind. Eng. Chem. Res. 38 (1999) 270–275.

[84] J.P. Hobson, Physical adsorption isotherms extending from ultrahigh vacuum to vapor pressure, J. Phys. Chem. 73 (1969) 2720–2727.

[85] M.J. Rosen, Surfactants and Interfacial Phenomena, John Wiley, New York, 1978.

[86] S. Lagergren, Zur theorie der sogenannten adsorption geloster stoffe, K. Sven. Vetenskapsakad. Handl. 24 (4) (1898) 1–39.

[87] Y.S. Ho, Citation review of Lagergren kinetic rate equation on adsorption reactions, Scientometrics 59 (2004) 171–177.

[88] Y.S. Ho, G. McKay, Kinetic models for the sorption of dye from aqueous solution by wood, Process Safety Environ. Prot. 76B (1998) 183–191.

[89] Y.S. Ho, G. McKay, A two-stage batch sorption optimized design for dye removal to minimum contact time, Process Safety Environ. Prot. 76B (1998) 313–318.

[90] Y.S. Ho, G. McKay, A comparison of chemisorption kinetic models applied to pollutant removal on various sorbents, Process Safety Environ. Prot. 76B (1998) 332–340.

[91] Y.S. Ho, G. McKay, The kinetics of sorption of basic dyes from aqueous solution by Sphagnum moss peat, Can. J. Chem. Eng. 76 (1998) 822–827.

[92] Y.S. Ho, G. McKay, Kinetic model for lead (II) sorption on to peat, Adsorpt. Sci. Technol. 16 (1998) 243–255.

[93] Y.S. Ho, G. McKay, Comparative sorption kinetic studies of dye and aromatic compounds onto fly ash, J. Environ. Sci. Health: Part A: Toxic/Hazard. Substances Environ. Eng. 34 (1999) 1179–1204.

[94] Y.S. Ho, G. McKay, Pseudo-second order model for sorption processes, Process Biochem. 34 (1999) 451–465.

[95] Y.S. Ho, G. McKay, A kinetic study of dye sorption by biosorbent waste product pith, Resour. Conserv. Recycl. 25 (1999) 171–193.

[96] Y.S. Ho, G. McKay, Batch lead (II) removal from aqueous solution by peat: equilibrium and kinetics, Process Safety Environ. Prot. 77B (1999) 165–173.

[97] Y.S. Ho, G. McKay, The kinetics of sorption of divalent metals ions onto sphagnum moss peat, Water Res. 34 (2000) 735–742.

[98] Y.S. Ho, G. McKay, Application of kinetic models to the sorption of copper (II) on to peat, Adsorpt. Sci. Technol. 20 (2000) 797–815.

[99] Y.S. Ho, G. McKay, Sorption of dye from aqueous solution by peat, Chem. Eng. J. 70 (1998) 115–124.

[100] V.C. Srivastava, M.M. Swamy, I.D. Mall, B. Prasad, I.M. Mishra, Adsorptive removal of phenol by bagasse fly ash and activated carbon: equilibrium kinetics and thermodynamics, Colloids Surf. A: Physicochem. Eng. Aspects 272 (2006) 89–104.

[101] G. McKay, M.S. Otterburn, J.A. Aga, Intraparticle diffusion process occurring during adsorption of dyestuffs, Water Air Soil Pollut. 36 (1987) 381–390.

[102] S. Goswami, U.C. Ghosh, Studies on adsorption behaviour of Cr(VI) onto synthetic hydrous stannic oxide, Water SA 31 (2005) 597–602.

[103] W.J. Weber, J.C. Morris, Kinetics of adsorption on carbon from solution, J. Sanitary Eng. Div.: Am. Soc. Civil Eng. 89 (SA2) (1963) 31–60.

[104] J.C. Morris, W.J. Weber, Removal of biologically-resistant pollutants from waste waters by adsorption, in: W.W. Eckanfelder (Ed.), Advances in Water Pollution Research, 2, Pergamon Press, London, 1964, pp. 231–266.

[105] B.M. Babic, S.K. Milonjic, M.J. Polovina, S. Cupic, B.V. Kaludjerovic, Adsorption of zinc cadmium and mercury ions from aqueous solutions on an activated carbon cloth, Carbon 40 (2002) 1109–1115.

[106] Y.H. Li, C.W. Lee, B.K. Gullett, The effect of activated carbon surface moisture on low temperature mercury adsorption, Carbon 40 (2002) 65–72.

[107] D. Mohan, V.K. Gupta, S.K. Srivastava, S. Chander, Kinetics of mercury adsorption from wastewater using activated carbon derived from fertilizer waste, Colloids Surf. A: Physicochem. Eng. Aspects 177 (2001) 169–181.

[108] C. Namasivayam, K. Kadirvelu, Uptake of mercury (II) from wastewater by activated carbon from an unwanted agricultural solid by-product: coirpith, Carbon 37 (1999) 79–84.

[109] K.D. Henning, K. Keldenicht, K. Knoblauch, J. Degel, Impregnated activated carbon for mercury removal, Gas Sep. Purif. 2 (1988) 20–22.

[110] J.V. Nabais, P.J.M. Carrott, M.M.L. Ribeiro Carrott, M. Belchior, D. Boavida, T. Diall, I. Gulyurtlu, Mercury removal from aqueous solution and flue gas by adsorption on activated carbon fibres, Appl. Surf. Sci. 252 (2006) 6046–6052.

[111] C. Namasivayam, D. Sangeetha, Recycling of agricultural solid waste, coir pith: removal of anions, heavy metals, organics and dyes from water by adsorption onto ZnCl$_2$ activated coir pith carbon, J. Hazard. Mater. 135 (2006) 449–452.

[112] A. Rubel, R. Andrews, R. Gonzalez, J. Groppo, T. Robl, Adsorption of Hg and NO$_X$ on coal by-products, Fuel 84 (2005) 911–916.

[113] M.M. Maroto-Valera, Y. Zhanga, E.J. Graniteb, Z. Tanga, H.W. Pennlineb, Effect of porous structure and surface functionality on the mercury capacity of a fly ash carbon and its activated sample, Fuel 84 (2005) 105–108.

[114] R. Yan, D.T. Liang, Leslie Tsen, Y.P. Wong, Y.K. Lee, Bench scale experimental evaluation of carbon performance on mercury vapour adsorption, Fuel 83 (2004) 2401–2409.

[115] H. Zenga, F. Jina, J. Guob, Removal of elemental mercury from coal combustion flue gas by chloride-impregnated activated carbon, Fuel 83 (2004) 143–146.

[116] S.-H. Lee, Y.-O. Park, Gas-phase mercury removal by carbon-based sorbents, Fuel Process. Technol. 84 (2003) 197–206.

[117] S. Vitolo, M. Seggiani, Mercury removal from geothermal exhaust gas by sulfur-impregnated and virgin activated carbons, Geothermics 31 (2002) 431–442.

[118] E. Ekinci, T. Budinova, F. Yardim, N. Petrov, M. Razvigorova, V. Minkova, Removal of mercury ion from aqueous solution by activated carbons obtained from biomass and coals, Fuel Process. Technol. 77–78 (2002) 437–443.

[119] K.A. Krishnan, T.S. Anirudhan, Removal of mercury (II) from aqueous solutions and chlor-alkali industry effluent by steam activated and sulphurised activated carbons prepared from bagasse pith: kinetic and equilibrium studies, J. Hazard. Mater. B92 (2002) 161–183.

[120] A.K. Bajpai, N. Vishwakarma, Adsorption of polyvinylalcohol onto Fuller's earth surfaces, Colloids Surf. A: Physicochem. Eng. Aspects 220 (2003) 117–130.

[121] J.F. Porter, G. McKay, K.H. Choy, The prediction of sorption from a binary mixture of acidic dyes using single- and mixed-isotherm variants of the ideal adsorbed solute theory, Chem. Eng. Sci. 54 (1999) 5863–5885.

[122] S.J. Allen, Q. Gan, R. Matthews, P.A. Johnson, Comparison of optimised isotherm models for basic dye adsorption by kudzu, Bioresour. Technol. 88 (2003) 143–152.

[123] G.E. Boyd, A.M. Adamson, L.S. Myers, The exchange adsorption of ions from aqueous solutions by organic zeolites, J. Am. Chem. Soc. 69 (1949) 2836.